ELSEVIER

International Journal of Mass Spectrometry 223–224 (2003) 271–278

International Journal of Mass Spectrometry

www.elsevier.com/locate/ijms

The ion extraction efficiency in a crossed beams experiment using a trochoidal electron monochromator

P. Cicman[a], M. Francis[b], J.D. Skalný[c], T.D. Märk[c,*]

[a] *Institut für Ionenphysik, Leopold Franzens Universität, Technikerstrasse 25, A-6020 Innsbruck, Austria*
[b] *Department of Physics and Engineering Physics, Stevens Institute of Technology, Hoboken, NJ 07030, USA*
[c] *Deptartment of Plasma Physics, Comenius University, Mlynska Dolina F2, 84215 Bratislava, Slovak Republic*

Received 1 February 2002; accepted 23 April 2002

Abstract

The ion extraction efficiency from a trochoidal electron monochromator was investigated for the same set-up as used in previous experiments. Using the Simion program the ion trajectories in the monochromator were simulated and the ratio of the extracted ions to all ions produced was estimated. The extraction efficiency was found to change very dramatically even at low ion energies, thus, deforming measured attachment cross sections. The results of the simulation were then applied to previously measured cross-section data for dissociative electron attachment to ozone. The corrected data showed very good agreement with the experiments of other authors. (Int J Mass Spectrom 223–224 (2003) 271–278)

Keywords: Electron monochromator; Ion extraction efficiency; Electron attachment cross section; Ozone

1. Introduction

The potentially most fruitful technique for the study of electron attachment is the crossed beam technique, which enables measurement of the cross-section of the production of selected ionic products. The total attachment cross sections, or more frequently the relative attachment cross sections, are measured using this method as a function of electron energy. A frequent problem of this technique is to achieve a minimum spread of the electron energy in the electron beam. This spread is characterized by the full-width at half-maximum (FWHM) in the distribution function. In order to achieve a small FWHM, a trochoidal electron monochromator (TEM) is a suitable device. The TEM was developed in the 1960s by Stamatovič and Schultz [1] and is used to select the electrons by their velocities (energies). In our laboratory, a TEM based on the original Stamatovič and Schultz design was built and used to perform measurements of electron attachment cross sections for several gases [2–5]. Such a design is very advantageous when processes at low electron energies are investigated, enabling us to work with a FWHM of the electron beam in the range of tens of meV.

Two important issues should be considered in detail. First, the TEM lens geometry should be optimized to minimize undesired electric field interactions. Such an optimization improves the stability of the electron current, thus, improving the electron energy resolution

* Corresponding author. E-mail: tilmann.maerk@uibk.ac.at

1387-3806/02/$ – see front matter
PII S1387-3806(02)00863-1

characteristics. This issue was examined in detail in recently published works [6,7]. Second, the ion extraction efficiency must also be considered, as it directly influences the experimental results. The operation of the TEM in the high energy resolution regime (tens of meV) requires the electric extraction fields in the collision chamber to be very small, in order to minimize electric field effects on the electron energy distribution function. In such a case, the extraction efficiency of the ionic fragments with higher kinetic energies is reduced, and the measured ion signal may not correspond to the rate of ion production in the collision chamber.

A typical example for such a problem is the case of dissociative electron attachment to ozone. This process is known to proceed in the gas phase through two channels:

$$e^- + O_3 \rightarrow O^- + O_2 \quad (1)$$

$$e^- + O_3 \rightarrow O_2{}^- + O \quad (2)$$

The production of O^- through channel (1) has first been reported by Curran [8] and later by Skalný et al. [9] having one resonance at 1.3 eV. Later, the existence of additional resonances at 3.5 and 7.5 eV was discovered by Walker et al. [10]. These additional resonances were later confirmed by the measurements of Allan et al. [11], Senn et al. [12], and Rangwala et al. [13]. The measurements of Walker et al. [10] showed that at resonances of 3.5 and 7.5 eV the O^- ions are created with significantly high kinetic energies (about 2 eV) while in case of the 1.3 eV resonance the kinetic energies were about 0.1 eV. As Skalný et al. [9] did not detect the 3.5 and 7.5 eV resonances and Senn et al. [12] detected only a very small signal at 3.5 and 7.5 eV resonances, this suggested some effects of ion discrimination in the TEM used.

In the present paper, the extraction efficiency of the ions from this TEM and its influence on the measured data is investigated. Extraction efficiencies of different fragment ions were simulated by the computer using the TEM geometry from these earlier experiments [9,12]. On the base of these results, earlier experimental data for dissociative electron attachment to ozone [12] are revised and this revised data then compared with the original results. A comparison of these results with the data of other authors is also presented.

2. Experimental set-up

The details of the experimental set-up of our crossed beam experiment were previously described, e.g., in [2–5,9,12]. For better understanding, the principle of the TEM used in previous experiments (also shown in Fig. 1) will be shortly described. In the TEM the electrons are produced by thermal emission from a hairpin filament directly heated by an electron current. The electron beam is formed by a system of three electrodes (pusher, anode and entrance) in the *x*-direction and enters the dispersion volume formed by crossed homogenous electric (*y*-directions) and magnetic fields (*x*-directions). In this region, the slow electrons are more strongly deflected in the *z*-direction and the quicker ones only slightly. Using an aperture with a diameter of 1 mm, electrons with a narrow energy spread are selected and by a system of two lenses accelerated or decelerated to an energy desired for a reaction in the collision chamber. After passing the collision chamber, the electrons are accelerated by two lenses and collected by a Faraday cup. In order to extract the ions to the mass spectrometer, an extraction field is applied between the electrodes in the reaction chamber. The extracted ions enter the quadrupole mass spectrometer and the selected ions are detected by channeltron.

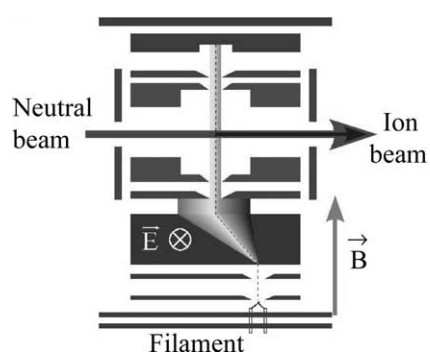

Fig. 1. A schematic view of the TEM.

3. Analysis of the extraction efficiency of the TEM

In this section we look in detail at the ion trajectories in the collision chamber of the TEM. The geometry of the collision chamber of the TEM together with the entrance lenses to the quadrupole mass spectrometer were simulated in three dimensions using a Simion program [14]. The electron–particle collision, or more accurately the creation of the negative ions, was assumed to take place in the geometrical middle of the collision chamber. The distribution of ion velocities in different directions was assumed to be isotropic. Then, from the point of the ion creation, the ions were assumed to move in the simulation in all directions (in steps of 0.5°, for ion kinetic energies in the range 0–10 eV). From such a simulation, the number of ions entering the quadrupole mass spectrometer has been calculated. The ratio of the ions entering the quadrupole to the number of all ions was taken as extraction efficiency for a given ion energy. This process was repeated for different ion energies in the range 0–10 eV as a function of the electric extraction potential up to 10 V.

Fig. 2 shows some results of the simulations, i.e., O^- ion trajectories in the collision chamber of the TEM and in the ion optics before the entrance to quadrupole mass spectrometer. For comparison, results are shown for two ion kinetic energies, 0.1 and 1 eV, when using two different extraction potentials (0.1 and 5 V). In order to measure ions from the collision chamber in the mass spectrometer no electric extraction field is in principle required. This is because the ions produced with velocity component in the narrow angle facing the spectrometer are able to get to the detector (not to mention the velocity of the neutral beam in direction of the mass spectrometer). Now, if an electric extraction field is applied, the number of detected ions increases with increasing extraction potential. This can be seen in Fig. 2 where just a fraction of ions with small kinetic energies enter the mass spectrometer for small extraction potential of 0.1 V (Fig. 2a), while all ions with small kinetic energies can reach the mass spectrometer for the high extraction potential of 5 V (Fig. 2c). In the case of ions with higher kinetic energies, such as 1 eV, the effect of extraction potential is also shown in Fig. 2b and d. For high kinetic energies the effect of extraction potential remains similar, hence increasing the extraction potential increases the number of detected ions. In this case, the number of detected ions is much smaller than in the case of lower ion energies and we are not able to extract all ions even for the high extraction potential of 5 V, as seen in Fig. 2d.

From the above results it follows that it could be easily possible to increase the extraction efficiency from the TEM simply by increasing the electric extraction field E. This can prove to be very advantageous when using gases with small electron attachment cross sections, where the negative ion signal is quite small. On the other hand, the use of the electric extraction field affects the electrons in the electron beam. First, the presence of an electric field in the collision region makes this region effectively another dispersion region with crossed E and B fields, which leads to the deflection of electrons. Second, the electric field in this region also causes a broadening of the electron distribution and a possible shift of the electron energy scale. It is then clear that the small extraction fields, and, thus, high electron energy resolution, is accompanied by the higher discrimination of the ionic products. Finding a reasonable compromise between the electron energy resolution and ion discrimination can in some cases be very difficult, as it directly determines the error and limitations of the cross-section measurements.

It should be noted, that even using the maximum number of grid points in the Simion program, the edges of the lens orifices can never be modeled precisely, which leads to the errors in the estimated electric field distribution inside the TEM. Also, the stepping of the starting angle for the ions is the source of another possible error in the final extraction efficiency. The effect of these errors is, however, small when compared with the calculated extraction efficiency.

Using the simulation described, the extraction efficiency of O^- and $O_2{}^-$ ions was analyzed. The results of the simulation are shown in Fig. 3. It is seen, that the

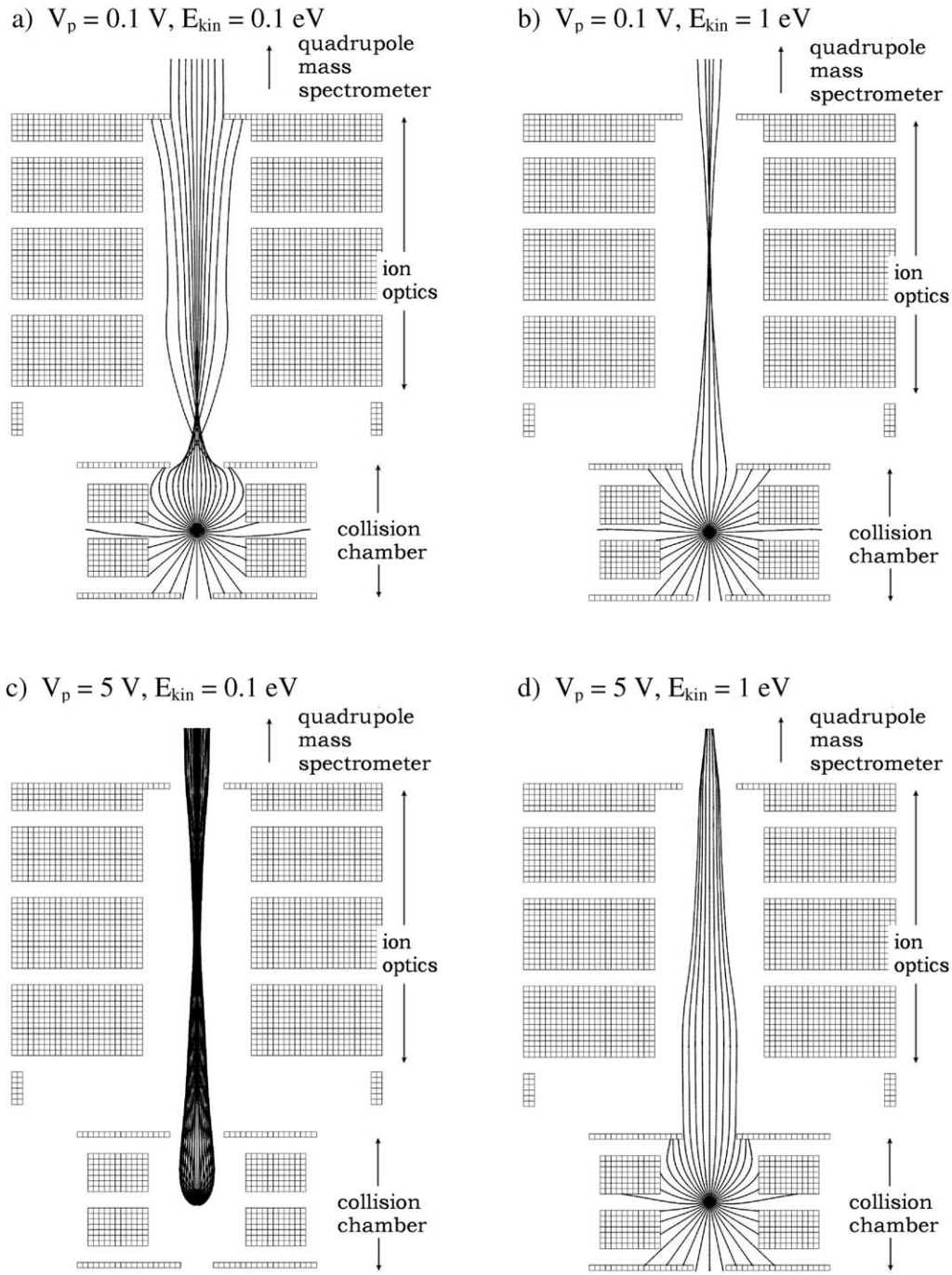

Fig. 2. Simulation of the ion trajectories for two different extraction potentials V_p and two different ion energies E_{kin}. The results are shown for O^- ions.

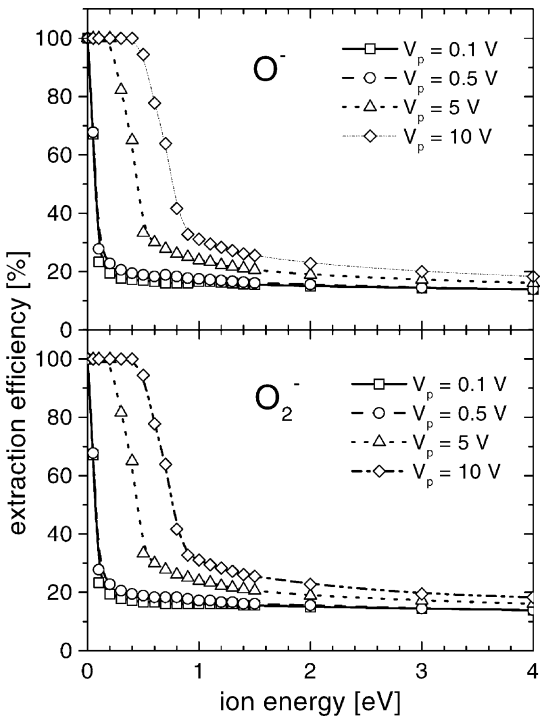

Fig. 3. Extraction efficiencies of O^- and $O_2{}^-$ ions for different extraction voltages V_p as a function of their kinetic energies.

results are almost identical for both O^- and $O_2{}^-$. In fact, the simulation was run also for higher ion masses (up to 100 amu) with similar results, as in Fig. 3.

For ions having kinetic energies smaller than about 0.4 eV the extraction efficiency is at its maximum (100%) when a high electric extraction field is applied. At higher ion energies the extraction efficiency is strongly reduced down to about 20%. In the case of low electric extraction field (extraction potential below 1 V) only a small fraction of ions can be extracted. Low extraction efficiency for low extraction fields indicates that when using the TEM, we are able to detect only ions, which are created with the initial velocity towards the detection system. All the other ions are lost to the collision chamber walls.

Under the conditions described above, the efficiency for the extraction of ions having higher kinetic energy is reduced non-linearly with the ion energy. Therefore, the experimentally measured yield of ions per time unit is not proportional to the rate of the ion formation in the collision region. Better to say, the shape of ion yield, measured as a function of electron energy, does not correspond to the real shape of the attachment cross section as a function of electron energy. Previously, when converting the measured ion yields to cross section values, this proportionality was thought to exist in our TEM [15].

4. Recalculation of the experimental data

In this section, the simulated extraction efficiencies will be used to correct the results of the previous experiments of dissociative electron attachment to ozone. In order to do so, the data on the kinetic energy release in process (1) and (2) are needed and were taken from the experiments of Walker et al. [10]. In their work, the ionic kinetic energy data was reported separately for different resonances of O^- and $O_2{}^-$ ion production. In order to use this data in present calculations, the measured ionic signal was separated by multi-peak fitting in order to obtain the corresponding cross-section component for each resonance. Then, knowing the ion energies for different resonances and corresponding ion discrimination for these energies, it was possible to correct the measured signal to account for the discrimination factor.

It should be noted that in the calculations, the most probable ion kinetic energies, derived from the ion energy distributions, were used, rather then ion distribution functions. This was because of quite low electron energy resolution (∼0.5 eV) in the experiment of Walker et al. [10]. Moreover, the sharp and narrow peak near 0 eV was not corrected because no data concerning ion energies in this process have been reported. However, as the peak position is very close to 0 eV, it was assumed that the ion kinetic energies are small; hence the extraction efficiency would be close to 100%.

Fig. 4 shows previously measured O^- and $O_2{}^-$ anion signal as a function of incident electron energy for electron energies up to 10 eV. Also, in Fig. 4 the ion signal corrected to account for the discrimination

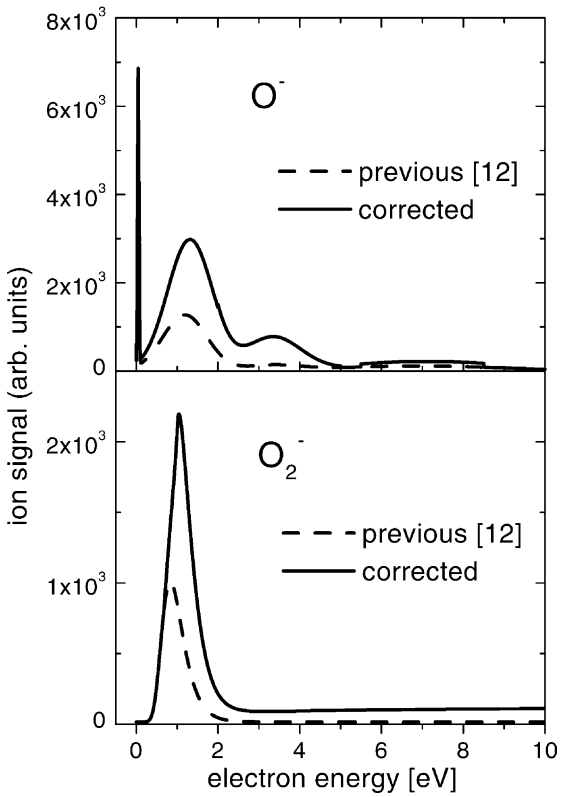

Fig. 4. O^- and $O_2{}^-$ signals for dissociative electron attachment to ozone as measured in our earlier measurements [12] and after the correction using the presently calculated ion extraction efficiencies.

is shown. A broad peak centered at about 1.3 eV for O^- and 1 eV for $O_2{}^-$ was found to be in excellent agreement with earlier experimental data [8,10,11]. The observation of a rather large and sharp peak close to zero energy in the measured O^- anion cross section has been already reported [12]. The height and width of this sharp peak was found to depend solely upon the incident electron beam resolution [12]. It is seen that the discrimination of the energetic ions causes significant decrease in the measured signal intensity, down to about half of the real intensity. On the other hand, the peak position of the major peak at 1 and 1.3 eV, respectively, does not change significantly in the case of O^- but shifts about 0.2 eV in the case of $O_2{}^-$. The shift in $O_2{}^-$ signal after correction, however, provides better agreement with the results of other authors, which justifies the presently applied procedure. A most significant effect of the ion discrimination can be seen for the resonance at electron energy of about 3.5 eV. Although, this resonance was also reported in our previous work [12], the signal intensity at this energy was much smaller (compared to the 1.2 eV signal), when compared with Walker et al. [10] and Rangwala et al. [13]. It was suggested in their work [13], that the difference between their data [13] and our older data [9,12] might be ascribed to the discrimination of the ions by their kinetic energies. As the measured O^- ion kinetic energy at 3.5 eV is around 2 eV [10], from Fig. 3 it then follows, that at this energy, we are able to detect only about 15% of the ions produced. This can be clearly seen in Fig. 4, where a very small signal from previous experiments becomes more relevant after the readjustments necessary due to the extraction efficiency of the TEM. On the other hand, the ability of Walker et al. [10] to extract and detect almost all ions in their experiment resulted in quite poor electron energy resolution. Therefore, they were not able to observe the resonance near 0 eV, whose detection was reported to be very sensitive to the electron energy resolution [12].

In addition, it might prove to be very useful to compare the estimation of the absolute attachment cross section with the data of other authors. This is shown in Fig. 5 for both ionic fragments (Fig. 5a and b) and total negative ion formation (Fig. 5c). The estimation of the absolute values of the cross section was done as follows. From the known ozone concentration and the measured peak heights of the O^- signal from O_3 (lower electron energies) and O^- from O_2 (at 6.5 eV) it was possible to calibrate absolutely the cross section scale, using known cross section for O^- production from O_2. With this method, the value for O^- production at 1.3 eV resonance was estimated in our previous experiment [12] as 2.8×10^{-17} cm^2 (see dashed line in Fig. 5a). Rangwala et al. [13] obtained at 1.3 eV the value 3.7×10^{-17} cm^2 by the same method. Although the agreement of these values may be considered quite good, we would like to point out one important consideration. In our previous experiment [12], the discrimination of O^- from O_3 and O^- from O_2 is different

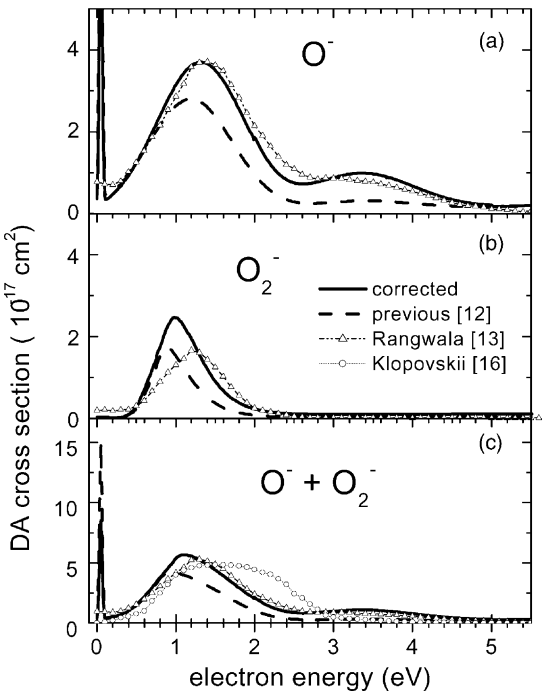

Fig. 5. Dissociative attachment cross section for O^- (a) and $O_2{}^-$ (b) negative ion production from ozone and their sum (c), compared with other results.

and, thus, increases the error in the calculation of the absolute value of the cross section. However, as Rangwala et al. [13] were able to collect all, low and high energetic ions, their estimation of the absolute cross section by the same method would provide more reliability. Therefore, in the present procedure, the data was calibrated to the O^- cross section values of Rangwalla et al. [13] of 3.7×10^{-17} cm^2 at 1.3 eV. Then, comparing the known signal of O^- to that of $O_2{}^-$ the value of cross section for $O_2{}^-$ ion formation at about 1 eV was obtained as 2.3×10^{-17} cm^2. This value is larger than 1.68×10^{-17} cm^2 of Rangwala et al. [13] (see Fig. 5b).

Despite these slight discrepancies, very good agreement of the present data with that of Rangwala et al. [13] is seen (in Fig. 5c), where the total attachment cross sections for the creation of the negative ions are shown. In this figure, the theoretical calculations of the cross section from Klopovskii et al. [16] are also shown. Very good agreement in the total attachment cross section is seen for the experimental data (except for the old data, which does not take into account the ion discrimination), while the theoretical calculations of Klopovskii et al. [16] show a much wider cross section with the maximum shifted to higher electron energy by about 0.5 eV. On the other hand, the experimental and theoretical estimation of the cross section values is in very good agreement. The experiments yield a maximum cross section values 5.65×10^{-17} cm^2 (present data), 4×10^{-17} cm^2 [12], 5.3×10^{-17} cm^2 [13] while the theoretical calculation gives 4.85×10^{-17} cm^2 [16]. Again, the value of 4×10^{-17} cm^2, estimated from previous experiment [12], is lower due to the negligence of the ion discrimination in the experiment.

Knowing the absolute cross section values for the dissociative electron attachment to ozone, as shown in (Fig. 5c), one can calculate the attachment rate coefficient k for this process using the formula

$$k = \sqrt{\frac{8}{\pi m_e}} \int_0^\infty \sigma(\varepsilon) \varepsilon_k^{-3/2} \varepsilon \exp\left[-\frac{\varepsilon}{\varepsilon_k}\right] d\varepsilon \qquad (3)$$

where m_e is the electron mass, $\sigma(\varepsilon)$ is the absolute attachment cross section, ε is the mean electron energy and $\varepsilon_k = (2/3)\varepsilon$. Then it is possible to compare the results of the cross section measurements with swarm experiments, where attachment rate constants can be directly measured.

Using Eq. (3), the thermal attachment rate constant from the present cross section data has a value of 1.7×10^{-9} cm^3 s^{-1}. The current data is fairly well consistent with the values of $k \geq 1 \times 10^{-9}$ cm^3 s^{-1} as determined by Kastelewitz and Bachman [17] and using low temperature gas discharge plasmas [18–20]. Also, from the attachment rate coefficient data obtained in oxygen–ozone [21] and air–ozone [22] mixtures in drift tubes, such values for the rate constant can be obtained. In contrast to these, low values of the thermal rate constant ($<1 \times 10^{-11}$ cm^3 s^{-1}) are typical for all earlier swarm data [23]. Also, the calculation of rate constant data reported by Klopovskii et al. [16] yields a value of 5×10^{-10} cm^3 s^{-1} close to the present one.

The presently reported results confirm the fact that dissociative electron attachment to ozone under certain conditions typical for low temperature gas discharges (mean energy close to 1 eV) is a process, which considerably contributes to the mechanism of ozone decomposition by electron impact. Therefore, this process must be considered, in addition to the direct electron impact dissociation, in the kinetic models of ozone formation by electrical discharges. More detailed study on the attachment coefficient for the dissociative electron attachment to ozone is in progress and will be published in the near future.

5. Conclusions

The revision of the experimental data from previous crossed beams experiments on dissociative electron attachment to ozone was reported. The conditions in the collision chamber of the TEM (where ions were produced) were simulated. The results of this simulation showed strong discrimination of the created ions due to their high kinetic energies. Therefore, the ion discrimination must be taken into account in the data analysis of this type of experiment, otherwise the results are strongly falsified. Using the results of this simulation, previous experimental data were corrected in account for the ion discrimination. The corrected results showed very good agreement with the experimental data of other authors. The calculation of the electron attachment rate constant is in very good agreement with the values obtained by experimental techniques using electrical discharges and is an order of magnitude higher than values measured in swarm techniques. These results suggest the role of electron attachment to ozone being more important that previously thought.

Acknowledgements

This work was supported by FWF, ÖAW, ÖNB, Wien, Austria and EU Commission, Brussels. JDS would like to thank for the support to Slovak Grant Agency Vega 2 under the project 1/765920.

References

[1] A. Stamatovič, G.J. Schultz, Rev. Sci. Instr. 41 (1969) 423.
[2] A. Kiendler, Š. Matejčík, J.D. Skalný, A. Stamatovič, T.D. Märk, J. Phys. B: Atom. Mol. Opt. Phys. 29 (1996) 6217.
[3] Š. Matejčík, A. Kiendler, P. Cicman, J. Skalný, P. Stampfli, E. Illenberger, Y. Chu, A. Stamatovič, T.D. Märk, Plasma Sources Sci. Technol. 6 (1997) 140.
[4] T.D. Märk, Š. Matejčík, A. Kiendler, P. Cicman, G. Senn, J. Skalný, P. Stampfli, E. Illenberger, Y. Chu and A. Stamatovič, Progress lecture at ESCAMPIG 96, Poprad, Slovakia, 1996 (Text of Invited Lecture), p. LXI.
[5] P. Cicman, G. Senn, G. Denifl, D. Muigg, J.D. Skalný, P. Lukáč, A. Stamatovič, T.D. Märk, Czech. J. Phys. 48 (1998) 1135.
[6] V. Grill, H. Drexel, W. Sailer, M. Lezius, T.D. Märk, Int. J. Mass. Spectrom. 205 (2001) 209.
[7] V. Grill, H. Drexel, W. Sailer, M. Lezius, T.D. Märk, J. Mass. Spectrom. 36 (2001) 151.
[8] R.K. Curran, J. Chem. Phys. 35 (1961) 1849.
[9] J.D. Skalný, S. Matejčík, A. Kiendler, A. Stamatovič, T.D. Märk, Chem. Phys. Lett. 255 (1996) 112.
[10] I.C. Walker, J.M. Gingell, N.J. Mason, G. Marston, J. Phys. B: Atom. Mol. Opt. Phys. 29 (1996) 4749.
[11] M. Allan, K.R. Asmis, D.B. Popovic, M. Stepanovic, N.J. Mason, J.A. Davies, J. Phys. B: Atom. Mol. Opt. Phys. 29 (1996) 4727.
[12] G. Senn, J.D. Skalný, A. Stamatovič, N.J. Mason, P. Scheier, T.D. Märk, Phys. Rev. Lett. 85 (1999) 5028.
[13] S.A. Rangwala, S.V.K. Kumar, E. Krishnakumar, N.J. Mason, J. Phys. B: Atom. Mol. Opt. Phys. 32 (1999) 3795.
[14] D.A. Dahl, Simion 3D version 6.0, Idaho National Engineering Laboratory, 1995.
[15] J.D. Skalný, S. Matejčík, T. Mikoviny, J. Vencko, G. Senn, A. Stamatovič, T.D. Märk, Int. J. Mass Spectrom. 205 (2001) 77.
[16] K.S. Klopovskii, N.A. Popov, O.V. Proshina, A.T. Rakhimov, T.V. Rakhimova, Plasma Phys. Reports 23 (2) (1997) 165.
[17] H. Kastelewitz, P. Bachman, Preprint 78–10, Akademie der Wissenschaften der DDR, zentralinistitu für Elekroneprhysik, 1978, see also Ref. in E. Eliason, Brown Boweri Forschungsbericht No. KLR 83-40C, 1985.
[18] V.I. Gibalov, A.B. Pravdin, M. Wronski, in: Proceedings of HAKONE II (International Symposium on High Pressure and Low Temperature Plasma Chemistry), Kazimierz nad Wisla, Poland (edit. Technical Univerity, Lublin, 1989), p. 68.
[19] L.E. Khvorostovskaya, V.A. Yankovsky, Contrib. Plasma Phys. 31 (1991) 71.
[20] J. Ráhel, M. Pavlík, L. Holubčík, V. Sobek, J.D. Skalný, Contrib. Plasma Phys. 39 (1999) 502.
[21] S. Kajita, S. Ushiroda, Y. Kondo, in: Proceedings of 21st ICPIG, vol. 4, Beograd, Yugoslavia, 1989, p. 662.
[22] Y. Kondo, S. Kajita, S. Ushiroda, in: Proceedings of the Third Workshop on Radiation Detectors and their Use, Ibaraki, Japan, 1988, p. 64.
[23] G.E. Caledonia, Chem. Rev. 75 (1975) 333.